LAWRENCE
LIVERMORE
NATIONAL
LABORATORY

UCRL-JRNL-216023

Effect of Wavefront Error on 10^-7 Contrast Measurements

J. W. Evans, G. Sommargren, B. Macintosh,
S. Severson, D. Dillon

October 10, 2005

Optics Letters

Disclaimer

Effect of Wavefront Error on 10^{-7} Contrast Measurements

Julia W. Evans*, Gary Sommargren†, Bruce A. Macintosh

Lawrence Livermore National Laboratory
7000 East Ave, Livermore, CA 94550

Scott Severson, Daren Dillon

UCO Lick Observatory, Laboratory for Adaptive Optics, University of California at Santa Cruz
1156 High St., Santa Cruz, CA, 95064

We have measured a contrast of $6.5 \cdot 10^{-8}$ from $10 - 25\lambda/D$ in visible light on the Extreme Adaptive Optics testbed using a shaped pupil for diffraction suppression. The testbed was designed with a minimal number of high-quality optics to ensure low wavefront error and uses a phase shifting diffraction interferometer for metrology. This level of contrast is within the regime needed for imaging young Jupiter-like planets, a primary application of high-contrast imaging. We have concluded that wavefront error, not pupil quality, is the limiting error source for improved contrast in our system.

OCIS codes: 010.1080,050.1220

The field of high-contrast imaging with adaptive wavefront control, known as Extreme Adaptive Optics (ExAO) has garnered increased interest as astronomers work to image planets around other stars. A system planning to image warm Jupiter-like planets will require a contrast of between 10^{-6} and 10^{-7} in the near-IR.[1] Entering the high-contrast regime requires suppressing diffraction and limiting or controlling wavefront errors.[2] In the baseline experiment presented here, wavefront error was minimized by optical design and construction rather than active control. We have demonstrated that visible light contrast of better than 10^{-7} is achievable in a laboratory setting without adaptive optics. We determined that wavefront error in the system limits the achievable contrast. Scaling this result to 1.6 micron light would improve contrast by approximately an order of magnitude as contrast in

a diffraction-suppressed regime scales with wavelength squared.[2] Current work involves the control of wavefront errors with adaptive optics.

The ExAO testbed was designed with a minimal number of high-quality optics to ensure end-to-end wavefront error would be small ($<$ 1.5 nm RMS). In initial high-contrast measurements active wavefront control was not required, allowing experiments to focus on suppressing diffraction, understanding the high-contrast regime and developing experimental methods for high-contrast imaging (i.e. controlling scattered light). In imaging mode, the testbed consists of a laser source (532 nm) passed through an optical fiber and a high-quality lens ($<$ 1 nm RMS over the 50-mm beam size). The beam passes through a pupil stop, reflects off a flat mirror, and is imaged onto a CCD sampled at $\sim$ 5 times the Nyquist limit (See Fig. 1). Diffraction is suppressed with a prolate spheroid shaped pupil.[3] The shaped pupil produces a region of high contrast sufficient for laboratory testing and has the advantage of not introducing additional phase aberrations.

In Phase Shifting Diffraction Interferometer (PSDI) mode, the testbed becomes an extremely accurate ($<$ 0.5 nm RMS absolute wavefront accuracy) optical metrology system. The PSDI was developed at LLNL for metrology of complex aspheric optics.[4] Briefly, a probe wavefront is injected from the upper single-mode fiber shown in Fig. 1. This passes through the system and is focused onto a reference pinhole embedded in a super polished flat mirror. Meanwhile, a coherent reference beam passes through the pinhole and interferes with the outgoing probe wavefront. The interference pattern is recorded at a CCD located at an arbitrary location along the optical axis. Using standard phase-shifting interferometer techniques, this produces a measurement of the wavefront at this location. This can then be numerically propagated to the plane of interest, such as the pupil plane. The resolution of the PSDI is limited by the aperture of the reference pinhole (in the focal plane). The effective resolution in the 10-mm aperture plane is $\sim$ 155 microns.

Contrast is defined as the ratio of the intensity in the region of interest (ROI) to the core intensity and can be measured directly in a far-field image. There are several error sources in high-contrast imaging that must be reduced to achieve good results: insufficient dynamic range, scattered light from the optical system, and CCD saturation effects. We will discuss the contrast achieved and two potential limiting error sources: shaped pupil performance and wavefront error.

The CCD in the ExAO system has a dynamic range of approximately four orders of magnitude. A contrast measurement of 10^{-7} can only be made as a composite of two or more images. The testbed is housed in an opaque enclosure, but scattered light from elements in the optical path must also be controlled. Neutral density (ND) filters are inserted before fiber launching to measure the unsaturated core. Attenuation is measured in real time with a power meter. When removed and the integration time is increased the CCD is highly

saturated. This effect is controlled by co-adding short exposures for longer integrations and using a focal plane mask. The slow $f/\#$ of our system (effectively $f/200$) allows us to move the far-field camera approximately 15 mm behind the focal plane without loss of contrast. A mirrored v-shaped beam block is introduced at the focal plane to block the core, but not the ROI.

Figure 2 is an image of the unsaturated core overlayed on the saturated image where the core would be if it were not blocked by the focal plane mask. The x-shape is characteristic of the shaped pupil, which produces a dark region along the horizontal axis of the image. Note that the unsaturated image is plotted on a log scale while the saturated image is on a linear scale. For analysis each data set of 10 frames is averaged and the corresponding averaged dark frame is subtracted. Then each image is scaled according to the measured attenuation from the ND and integration time to be comparable with the saturated image. All of the images are normalized to the peak of the scaled unsaturated image.

The dark region in the saturated image is clearly visible on the right hand side of Fig. 2. In the region from $8 - 15\lambda/D$ the radial average contrast over 8 degrees is $1.3 \cdot 10^{-7}$ with an intensity variation of $1.0 \cdot 10^{-7}$. Over the larger region from $10 - 25\lambda/D$ the radial average contrast is $6.5 \cdot 10^{-8}$ with an intensity variation of $2.9 \cdot 10^{-8}$ (See the region indicated in Fig. 2). A substantial region in the PSF has better than 10^{-7} contrast, meeting the specifications for a current generation ground-based planet imager. The noise floor due to scattered light and CCD noise is measured to be below 10^{-8} behind the focal plane mask in the saturated image. It should be emphasized that the system is not noise limited (See Fig. 3).

When considering shaped pupil performance there are two areas to be examined: design and implementation. The design of shaped pupils is not new; Jacquinot and Dossier[5] give a description of early efforts in this area. With advances in computing and manufacturing these designs can be further optimized and realized.[6] We chose a simple single opening prolate spheroid pupil for our tests. This 10-mm diameter pupil was designed to have contrast of 10^{-10}, but a specification error lead to a deviation of 0.02-mm RMS from the desired points defining the opening. In simulation the resulting loss of contrast from this error is significant (~ 2 orders of magnitude) but below loss due to wavefront error (See Fig. 4).

The performance of a shaped pupil is also affected by its edge quality. Pupils manufactured by machining and lithographic etching were tested. Fig. 3 is a composite of radial averages from three images for each pupil. The normalized intensity of the unsaturated core of the etched pupil result does not quite align with the ROI measured in the saturated image due to saturation in the second image of the core composite. Over the ROI, the etched mask has an improvement of approximately 0.5 orders of magnitude over the machined mask. For achieving 10^{-6} contrast, the machined mask is more than adequate at our level of wavefront error and considerably less expensive to make. Comparing microscope images of the masks,

the machined pupil has an RMS edge quality roughly 3 times larger than the etched pupil. Wavefront quality is the same for both measurements indicating the machined pupil is limited by edge quality.

We also investigated the effect of wavefront error on high-contrast measurements. Using the PSDI we can accurately measure wavefronts and use the measurements to simulate expected far-field performance. This experiment has a total RMS wavefront error of 1.5 nm. That error breaks down to 0.5-nm astigmatism, 0.5-nm "ringing" (an artifact from the measurement), 0.3-nm spherical, 0.94-nm other mid-frequency and 0.7-nm high-frequency aberrations. The truncation effect at the PSDI reference pinhole, which causes ringing in the wavefronts, also causes the far-field simulation to break down at approximately $26\lambda/D$. To test if contrast is limited by wavefront error a series of simulations were done. Fig. 4 is a summary of those results.

To simulate the effect of wavefront error, we used measured wavefront error and generated a simulated mask from the points used to manufacture the physical mask (with the specification error included). This simulated mask does not include edge roughness. Radial averages over the ROI are plotted in Fig. 4. Good correspondence between experimental and simulated contrast indicates that edge roughness is not a significant factor with the etched mask. When comparing performance without phase errors, the ideal mask would perform several orders of magnitude better. In the current experimental set-up, however, even if wavefront error were reduced to 0.35 nm RMS, contrast would still be primarily wavefront error limited. The ideal mask when used with the reduced wavefront error would have better performance at large radii but not an overall improvement in contrast level. Significant mask errors need to be avoided to achieve better than 10^{-8} contrast. To operate in the contrast regime of 10^{-10}, wavefront error and mask quality will be critical. In the contrast regime needed for our experiments, however, wavefront error is the more prominent error source.

We have demonstrated that better than 10^{-7} contrast in visible light can be achieved in a laboratory setting with low-wavefront error and an etched shaped pupil. In the contrast regime of our tests, low wavefront error is more critical and more difficult to achieve than producing an adequate pupil for diffraction suppression. For the 10^{-6} contrast regime an inexpensive pupil could be substituted, provided wavefront error was adequately controlled. As wavefront error is the primary limitation to contrast, the next step is to implement active wavefront control. Tests using a MEMS deformable mirror for active wavefront control are ongoing.

Contact Julia Evans at `evans74@llnl.gov`. The authors would like to thank Don Phillion and Don Gavel. This work has been supported by the Gordon and Betty Moore Foundation through its grant to the UCO/Lick Observatory Laboratory for Adaptive Optics and the NSF Science and Technology Center for Adaptive Optics, managed by the Univer-

sity of California at Santa Cruz under cooperative agreement No. AST-9876783. This work was performed under the auspices of the U.S. Department of Energy by the University of California, Lawrence Livermore National Laboratory under contract No. W-7405-Eng-48.

*P.h.D. candidate at University of California, Davis

†Gary Sommargren 1944-2005

References

1. A. Burrows, M. Marley, W. B. Hubbard, J. I. Lunine, T. Guillot, D. Saumon, R. Freedman, D. Sudarsky, and C. Sharp, Astrophysical Journal **491**, 856 (1997).
2. A. Sivaramakrishnan, J. P. Lloyd, P. E. Hodge, and B. A. Macintosh, Astrophysical Journal **581**, L59 (2002).
3. N. J. Kasdin, R. J. Vanderbei, D. N. Spergel, and M. G. Littman, Astrophysical Journal **582**(2), 1147.
4. G. E. Sommargren, D. W. Phillion, M. A. Johnson, N. Q. Nguyen, A. Barty, F. J. Snell, D. R. Dillon, and L. S. Bradsher, in *Emerging Lithographic Technologies VI*, R. L. Engelstad, ed., Proc. SPIE **4688**, pp. 316 (2002).
5. P. Jacquinot and B. Roizen-Dossier, *Progress in Optics*, vol. 3, chap. Apodisation, pp. 31 (North-Holland Publishing Company-Amsterdam, 1964).
6. J. N. Kasdin, R. J. Vanderbei, M. G. Littman, and D. N. Spergel, Applied Optics **44**, 1117.

List of Figures

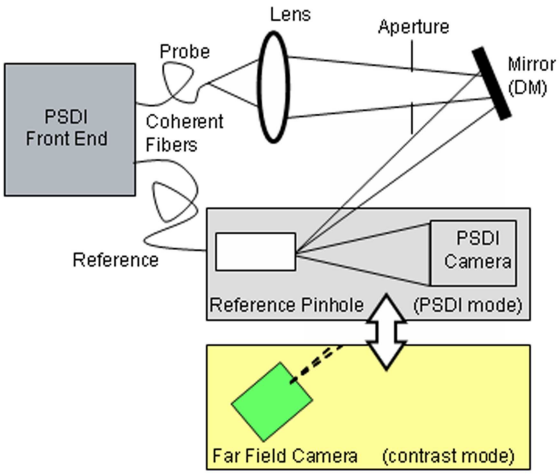

Fig. 1. Simplified schematic of the ExAO testbed. The Testbed has two modes of operation: Imaging and PSDI. The fold mirror in the system can be replaced with a deformable mirror for active wavefront control.

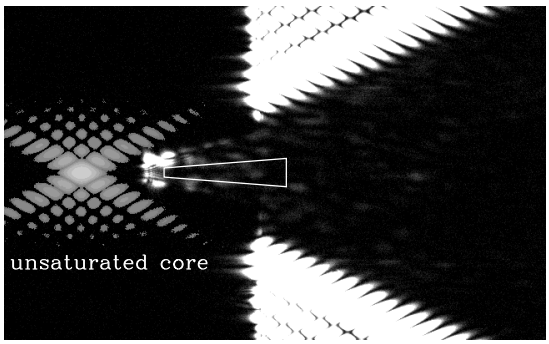

Fig. 2. An image of the unsaturated core overlayed on the saturated image where the core would be if it were not blocked by the focal plane mask. The x-shaped pattern is characteristic of the shaped pupil. The boxed area indicates the region of interest from $10 - 25\lambda/D$. These images are superimposed with different scales.

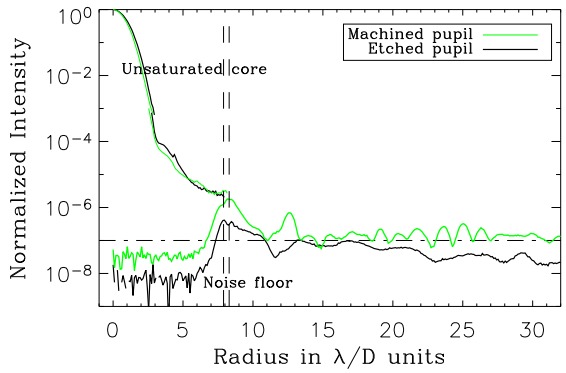

Fig. 3. Composite radial-average normalized-intensity far-field measurements made with the etched and machined shaped pupils. The vertical lines indicate the edge of the focal plane mask in the two tests. The noise floor behind the focal plane mask is below 10^{-8}.

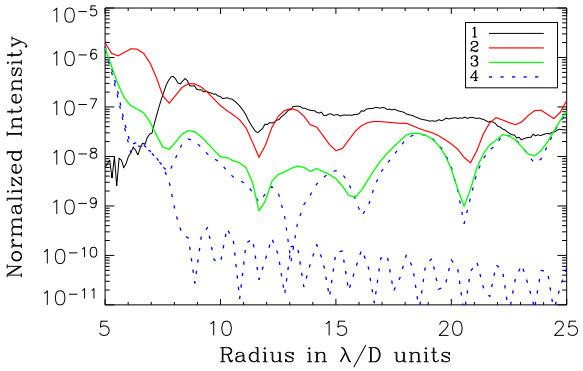

Fig. 4. Comparison of experimental results with results simulated with the pupil mask and various wavefront errors. Line 1 is the experimentally measured far-field contrast (as in Fig. 3). Line 2 is a far-field simulation using the experimentally measured phase and a shaped pupil mask with the same specification error as the physical mask. Line 3 is a simulation with the wavefront error reduced to 0.35 nm RMS and same flawed mask. The top line 4 is a simulation with no phase error and the flawed mask while the bottom line 4 is a no phase error and a perfect mask.